A Virus-Induced Gene-Silencing Vector Based on a Mild Isolate of Watermelon Mosaic Virus for Reverse Genetic Analyses in Cucurbits

Fakhreddine Houhou
IBMCP (CSIC-UPV), Valencia
Verónica Aragonés
IBMCP (CSIC-UPV), Valencia
Anamarija Butković
IBMCP (CSIC-UPV), Valencia
Cristina Sáez
COMAV, UPV, Valencia
Belén Picó
COMAV, UPV, Valencia
Carmelo López
COMAV, UPV, Valencia
José-Antonio Daròs (jadaros@ibmcp.upv.es)
IBMCP (CSIC-UPV), Valencia https://orcid.org/0000-0002-6535-2889

Research Article

Keywords: Virus-induced gene silencing, reverse genetics, melon, watermelon mosaic virus, cucurbit

Posted Date: February 17th, 2021

DOI: https://doi.org/10.21203/rs.3.rs-222617/v1

A virus-induced gene-silencing vector based on a mild isolate of *Watermelon mosaic virus* for reverse genetic analyses in cucurbits

Fakhreddine Houhou[1], Verónica Aragonés[1], Anamarija Butković[1], Cristina Sáez[2], Belén Picó[2], Carmelo López[2], José-Antonio Daròs[1,*]

[1]Instituto de Biología Molecular y Celular de Plantas (Consejo Superior de Investigaciones Científicas-Universitat Politècnica de València), Avenida de los Naranjos s/n, 46022 Valencia, Spain

[2]Instituto de Conservación y Mejora de la Agrodiversidad Valenciana, Universitat Politècnica de València, Avenida de los Naranjos s/n, 46022 Valencia, Spain

*To whom correspondence should be addressed: José-Antonio Daròs, jadaros@ibmcp.upv.es

Fakhreddine Houhou: http://orcid.org/0000-0002-2827-3102
Verónica Aragonés: http://orcid.org/0000-0002-4695-7890
Anamarija Butković: http://orcid.org/0000-0002-1435-0912
Cristina Sáez: http://orcid.org/0000-0003-4061-5758
Belén Picó: http://orcid.org/0000-0001-7761-990X
Carmelo López: http://orcid.org/0000-0001-7459-1315
José-Antonio Daròs: http://orcid.org/0000-0002-6535-2889

Abstract

Key message. A virus-induced gene silencing vector based on a mild isolate of watermelon mosaic virus (*Potyvirus*) facilitates reverse genetic analyses in cucurbits

Abstract. As a response to viral infections, host plants trigger an RNA-mediated gene silencing defense, to which viruses respond with the expression of viral-encoded RNA silencing suppressors. If virus clones are manipulated to include sequences homologous to host endogenous genes, these are also targeted by the plant RNA silencing machinery. This so-called

virus-induced gene silencing (VIGS) has become a powerful technique for reverse genetic analyses in plants, as an alternative to labor-intensive genome transformation. We show that a mild isolate of *Watermelon mosaic virus* (WMV, genus *Potyvirus*) can be used as a VIGS vector for reverse genetic analyses in melon. Recombinant WMV clones —in which fragments of the melon *Phytoene desaturase* (*PDS*) mRNA were inserted in sense, antisense, and hairpin modalities— induced a distinctive phenotype and significant silencing of the endogenous gene. While the foreign fragments in sense and antisense orientations were stable in the viral progeny, the hairpin was quickly lost. Nevertheless, the hairpin construct triggered a maintained silencing effect comparable to those of the sense and antisense constructs. The suitability of WMV as a VIGS vector was further confirmed targeting melon *Magnesium chelatase subunit I* (*CHLI*). These results also support that, although potyviruses express a strong silencing suppressor that usually precludes VIGS, mild isolates of this kind of viruses can be used as VIGS vectors. Finally, to facilitate the use of this new tool by cucurbit geneticists, we describe plasmid pGWMV-VIGS that allows easy cloning fragments of the genes of interest in a single Gibson assembly reaction.

Keywords: Virus-induced gene silencing, reverse genetics, melon, watermelon mosaic virus, cucurbit

Introduction

In most eukaryotic organisms, multiple pathways of RNA-induced gene silencing contribute to crucial biological functions such as development regulation, genome integrity, or responses to biotic and abiotic stresses. In plants, among these relevant roles, RNA silencing has been revealed as a foremost antiviral mechanism, since virtually all plant viruses encode one or more RNA silencing suppressors in their small genomes to accomplish infection (Csorba et al. 2015). Double-stranded RNA (dsRNA) replication intermediates from RNA viruses, as well as structured or overlapping transcripts from both RNA and DNA viruses, are recognized by the host plant Dicer-like (DCL) RNase III enzymes, which produce duplex small interfering RNAs (siRNAs) of approximately 20-24 nucleotides (nt). A single siRNA strand is loaded by an Argonaute (AGO) RNase H enzyme to form the RNA-induced silencing complex (RISC), which inactivates the viral nucleic acids—usually by cleavage, but also by translation arrest or DNA hypermethylation. Importantly, in plants, primary siRNAs can also serve as primers for the host RNA-dependent RNA polymerases to amplify the silencing signal by producing new

viral dsRNAs that are subsequently processed by DCLs to generate abundant secondary siRNAs to feed AGOs. siRNAs also contribute to systemic signaling of infection. This mechanism of antiviral RNA silencing implies that, if a sequence fragment homologous to a plant gene is artificially inserted into the viral genome, the host antiviral machinery will produce siRNAs that will also target the endogenous gene. Therefore, in reverse genetic analyses to study gene function, a relatively-simply built recombinant virus infectious clone can be used as an alternative to cumbersome plant genome transformation (Baulcombe 1999)—provided that the virus-encoded RNA silencing suppressors do not fully dismantle the host antiviral response, which is why viruses with mild or weak RNA silencing suppressors are preferred. This so-called virus-induced gene silencing (VIGS) was demonstrated more than two decades ago using both RNA and DNA plant viruses (Lindbo et al. 1993; Kumagai et al. 1995; Kjemtrup et al. 1998; Teresa Ruiz et al. 1998; Jones et al. 1998). Since then, it has been extensively applied to both model species (Liu et al. 2002b; Burch-Smith et al. 2006) and cultivars of agronomical interest (Holzberg et al. 2002; Liu et al. 2002a; Fofana et al. 2004). Recent reviews have comprehensively overviewed the more-than-fifty VIGS vector systems that have been developed to date, as well as the dicot and monocot species to which they can be applied (Kant and Dasgupta 2019; Dommes et al. 2019; Courdavault et al. 2020). However, despite the numerous currently available VIGS vectors, no universal system exists, since each plant virus (or even each virus strain) exhibits a particular host range and other biological peculiarities; therefore, novel systems are still required to efficiently target various plant species and families.

Potyviruses (genus *Potyvirus*, family *Potyviridae*) are the largest group of plant RNA viruses, with approximately 200 species currently recognized (Wylie et al. 2017). However, relatively few VIGS vectors have been derived from potyviruses (Lindbo et al. 1993; Gammelgård et al. 2007). This is possibly because potyviruses express a strong RNA-silencing suppressor: the helper-component protease (HC-Pro), which efficiently inhibits the host RNA-based antiviral response (Valli et al. 2018). In addition, the approximately 10,000-nt potyvirus RNA genome encodes a large polyprotein that, after translation, is processed in a regulated cascade by three virus-encoded proteases: P1 protease, HC-Pro, and the nuclear inclusion *a* (NIa) protease (NIaPro) (Revers and García 2015). Shorter polyprotein versions are also produced by transcriptional slippage mechanisms (Olspert et al. 2016). This genome organization, based on a nearly genome-long open reading frame (ORF), may have also hindered the development of VIGS vectors from potyviruses, since care must be taken to avoid interrupting the viral polyprotein with stop codons from exogenous sequences.

We have recently characterized a *Watermelon mosaic virus* (WMV, genus *Potyvirus*) isolate that induces mild symptoms in melon (*Cucumis melo* L.) and other cucurbits (Aragonés et al. 2019). WMV is one of the most prevalent viruses on cucurbits worldwide and exhibits a wide host range (Bertin et al. 2020; Desbiez et al. 2020). We investigated whether an infectious clone derived from this mild WMV isolate could be useful as a VIGS vector. The family *Cucurbitaceae* ranks second, after *Solanaceae*, in its economic importance in horticulture (Weng et al. 2020); it includes at least ten species considered major crops worldwide and more than twenty additional of local commercial importance (Chomicki et al. 2020). Again, few VIGS vectors have been developed for reverse genetics analyses in cucurbits (Igarashi et al. 2009; Zhao et al. 2016; Liu et al. 2020). In this work, we aim to derive a VIGS vector from a mild isolate of the potyvirus WMV for application in genetic analyses in cucurbits and for illuminating how fragments of host genes can be inserted into a potyvirus vector to efficiently induce gene silencing. In this way, we sought to not only add a new VIGS vector for cucurbits, but also to contribute to the incorporation of the highly diverse group of potyviruses into VIGS technology.

Materials and Methods

Plasmid construction

Plasmid pGWMV-Vera (Fig. S1) contains an infectious clone of the WMV Vera isolate (GenBank accession number MH469650) inserted in the binary plasmid pG35Z (Cordero et al. 2017), under the control of the CaMV 35S promoter and terminator (Aragonés et al. 2019). We amplified a fragment of this plasmid by the polymerase chain reaction (PCR) using primers P1 and P2, which contained flanking *Bsa*I restriction sites; this fragment was ligated to a basic cloning vector using T4 DNA ligase (Thermo Scientific). All PCRs for cloning purposes consisted of 30 cycles and were performed with Phusion high-fidelity DNA polymerase in buffer HF (Thermo Scientific). The sequences of the resulting plasmids were confirmed experimentally. The sequences of all primers used in our study are given in Table S1. The resulting plasmid, with a fragment of pGWMV-Vera, was linearized by PCR using primers P3 and P4 with extended 5' regions, in order to introduce the artificial NIaPro cleavage site at the NIb/CP intercistronic site. The PCR product was ligated to a linker consisting of two unique *Nhe*I and *Spe*I restriction sites flanking a *LacZ'* blue/white selection marker. We named the resulting intermediate plasmid pMWMV-Z (Fig. S1). Plasmids pGWMV-sPDS, pGWMV-

aPDS, pGWMV-hPDS, and pGWMV-sCHLI (Fig. S1) were constructed by two consecutive Gibson assembly reactions (Gibson et al. 2009), using the NEBuilder HiFi DNA assembly master mix (New England Biolabs). We amplified fragments of the melon (*Cucumis melo* L., cv. Piñonet Piel de Sapo) *Phytoene desaturase* (*PDS*; Cucurbit Genomics Database MELO3C017772.2), *Magnesium chelatase subunit I* (*CHLI*; MELO3C007233.2) genes by PCR using primers P5-P10 and P13-P16 (Table S1). The *Tetrahymena thermophila* 26S rRNA group-I self-splicing intron with 10-nt flanking exons (from positions 43 through 475 of GenBank accession no. V01416.1) was amplified with primers P11 and P12 from a cDNA template obtained by gene synthesis. The resulting intermediate plasmids were digested with *Bsa*I (BsaI-HFv2, New England Biolabs); the inserts were transferred to pGWMV-Vera digested with *Bpu*1102I and *Apa*I (Thermo Scientific) by means of a second Gibson assembly reaction. We created pGWMV-VIGS (Fig. S1) in a similar way, albeit by using primers P17 and P18.

Plant inoculation

Fifteen-day-old melon plants of the Piñonet Piel de Sapo cultivar were inoculated in the first true leaf with preparations of *Agrobacterium tumefaciens* C58C1 bearing the various WMV constructs. *A. tumefaciens* were previously transformed with helper plasmid pCLEAN-S48 (Thole et al. 2007). Transformed *A. tumefaciens* were selected at 28ºC in plates with 50 µg/l rifampicin, 7.5 µg/l tetracycline, and 50 µg/l kanamycin. Single colonies were then grown at 28ºC in liquid Luria-Bertani (LB) cultures containing, as a selection antibiotic, only 50 µg/l kanamycin. The various *A. tumefaciens* clones were harvested by centrifugation at an optic density at 600 nm (OD_{600}) between 0.5 and 2. The bacteria were resuspended in inoculation buffer (10 mM 2-(*N*-morpholino)ethanesulfonic acid (MES)-NaOH pH 5.6, 10 mM $MgCl_2$, and 150 µM acetosyringone) at OD_{600} 0.5. Virulence genes were induced by incubation for 3 h at 28ºC. Finally, induced bacteria were infiltrated in the abaxial side of the first true leaf of melon plants, using a needle-less 1 ml syringe. The plants were cultivated in a greenhouse at 25ºC with a 16-hour day and an 8-hour night photoperiod.

RNA analyses

At the indicated days post-inoculation (dpi), RNA was purified from systemic non-inoculated leaf tissue samples. Frozen leaf samples (approximately 50 mg) were ground in 2-ml Eppendorf

tubes, using a bead mill homogenizer (VWR) with 4-mm diameter stainless steel balls for 1 min at 30 s^{-1}. Aliquots of 1 ml of extraction buffer (4 M guanidine thiocyanate, 0.1 M sodium acetate, pH 5.5, 10 mM ethylenediaminetetraacetic acid —EDTA—, and 0.1 M 2-mercaptoethanol) were added to the tubes, which were vortexed intensively. The extracts were clarified by centrifugation for 5 min. We mixed 0.6 ml of the supernatant with 0.39 ml of 96% ethanol. After 1 mine of centrifugation, we loaded 0.7 ml of the supernatant on silica gel spin columns (Zymo-Spin I column, Zymo Research). The spin columns were washed twice with 0.5 ml of washing buffer (70% ethanol, 10 mM sodium acetate, pH 5.5); the RNA samples were eluted with 10 µl of 20 mM Tris-HCl, pH 8.5.

We performed WMV diagnosis using reverse transcription (RT)-PCR amplification followed by electrophoretic separation of the amplified products. Aliquots of 1 µl of RNA were subjected to RT with RevertAid reverse transcriptase (Thermo Scientific) using primer P19. Aliquots of 1 µl of the RT products were amplified by PCR for 30 cycles with *Thermus thermophilus* DNA polymerase (Biotools), using 1 µM primers P20 and P21 in 75 mM Tris-HCl, pH 9.0, 2 mM $MgCl_2$, 50 mM KCl, 20 mM $(NH_4)_2SO_4$, and 0.2 mM dNTPs. We electrophoresed the PCR products through a 1% agarose gel in buffer TAE (40 mM Tris, 20 mM sodium acetate, and 1 mM EDTA, pH 7.2). The gels were stained by shaking for 15 min in 0.5 µg/ml ethidium bromide. Viral progeny analysis at the NIb/CP intercistronic site was also performed by RT-PCR, followed by electrophoresis. RT was performed as explained above, albeit with primer P22. The PCR products were obtained with Phusion high-fidelity DNA polymerase, using primers P23 and P24, and analyzed by electrophoresis as explained above.

mRNA quantification

We quantified *PDS* and *CHLI* mRNAs using RT-quantitative PCR (qPCR). RNA was purified from leaf samples using Extrazol (BLIRT) and quantified using a NanoDrop 1000 spectrophotometer (Thermo Scientific). Remains of DNA were further removed using Perfecta DNase I (Qantabio). We analyzed three biological replicates and two technical replicates for each virus inoculum, using a LightCycler 480 system (Roche). The RT reactions were performed as explained above using an oligo(dT) primer. Aliquots of 1.5 µl of the RT products were used in the qPCR reactions in a final volume of 15 µl. We used 7.5 µl of 2 × FastStart Essential DNA Green Master (Roche), 1.5 µl 100 nM each primer and 1.5 µl of H_2O. We used primers P25-P26, P27-P28, and P29-P30 to amplify, respectively, fragments of *PDS*, *CHLI*,

and the housekeeping gene (*Cyclophilin CYP7*; MELO3C025848.2) (Gonzalez-Ibeas et al. 2007). The conditions consisted of an incubation for 5 min at 95ºC followed by 40 cycles of 5 s at 95ºC, 30 s at 60°C, and 15 s at 72ºC. Relative mRNA levels were calculated using the $2^{-\Delta\Delta Ct}$ method (Livak and Schmittgen 2001), where ΔΔCt is the difference between the ΔCt of each sample (ΔCt sample = Ct viral target gene – Ct housekeeping gene) and the ΔCt of the reference sample (ΔCt calibrator). The sample with lower ΔCt was used as the reference in both assays.

Results

Construction of a VIGS vector for reverse genetics analyses in cucurbits from a mild isolate of WMV

The Vera isolate of WMV (GenBank accession number MH469650) induces mild symptoms in commercial melon varieties, such as the Mediterranean elite Piel de Sapo cultivars (Aragonés et al. 2019). To study the potential use of this virus isolate for analyzing gene function in melon and other cucurbits, we used an infectious clone of this virus isolate as a vector to express fragments of the melon *Phytoene desaturase* (*PDS*). PDS is the second enzyme in the carotenoid biosynthesis pathway; its silencing is usually easily observed as a visual photobleaching phenotype. We expressed *PDS* mRNA fragments between the WMV nuclear inclusion *b* (NIb) and coat protein (CP) cistrons (Fig. 1), as this is a typical position to express foreign genes using potyvirus vectors (Choi et al. 2000). To avoid potential interference with virus infection, we also flanked the exogenous sequence with the two parts of an artificial NIaPro cleavage site to ultimately release the foreign fragment from the viral polyprotein (Fig. 1). Finally, to study the effect of the insertion on gene silencing, but also on vector stability, we expressed the *PDS* fragment in sense, antisense, and hairpin modalities (Fig. 1). In the latter case, we placed the inverted repeats that would produce both hairpin strands separated by the *Tetrahymena thermophila* rRNA group-I self-splicing intron, flanked by two 10-nt exon fragments—because it is well-known that DNA inverted repeats are highly unstable during plasmid amplification in *Escherichia coli*, unless they are separated with a spacer (Lai et al. 2016). Of course, our designs avoided the introduction of stop codons in the open reading frame of WMV polyprotein.

To prepare the vector system, beginning with the cloned WMV-Vera cDNA in plasmid pGWMV-Vera (Fig. S1), we transferred the final fragment of the WMV cDNA—including part

of NIb, the entire CP, and 3' UTR, as well as the 35S *Cauliflower mosaic virus* (CaMV) terminator—to a basic cloning vector. This DNA fragment was flanked by two *Bsa*I restriction sites to facilitate subsequent restoration, after manipulation, in pGWMV-Vera. Next, between the NIb and CP cistrons, we inserted the artificial NIaPro cleavage site, interrupted by a polylinker for cloning purposes. We named this intermediate plasmid pMWMV-Z (Fig. S1). The inserted artificial (-8/+3) NIaPro cleavage site corresponded to the native NIb/CP cleavage site, although it included silent mutations to avoid long sequence repetitions that would facilitate recombination during virus replication (Fig. 1 and Fig. S1). Next, we built the three intermediate plasmids to express fragments of the melon *PDS*: (i) the 5' 201-nt of the ORF in a sense orientation; (ii) the 5' 200-nt of the ORF in an antisense orientation, plus an additional T (we moved the reading frame +1 to avoid stop codons; and (iii) the 5' 102-nt of the ORF in a sense orientation, followed by the *T. thermophila* rRNA group-I intron and the 5' 101-nt of the ORF in an antisense-orientation, plus an additional T; again, we moved the ORF +1 to avoid stop codons (Fig. S2). Finally, these manipulated fragments of the WMV genome were transferred to pGWMV-Vera to create pGWMV-sPDS, pGWMV-aPDS, and pGWMV-hPDS (Fig. 1 and Fig. S1), in order to express *PDS* fragments in sense, antisense, and hairpin modalities, respectively.

Gene silencing of melon marker genes using the WMV vector

Triplicate young melon plants were agroinoculated in the first true leaves to express WMV-sPDS, WMV-aPDS, and WMV-hPDS. As controls, plants were also inoculated with *Agrobacterium tumefaciens* transformed with pG35Z (Supplementary Fig. S1)—the empty plasmid—and with pGWMV-Vera, the wild-type virus. Two weeks after inoculation, all melon plants, except those mock-inoculated with the empty plasmid, showed symptoms of infection. Interestingly, while plants inoculated with the WMV-Vera control exhibited the mild symptoms previously observed, plants inoculated with WMV-sPDS, WMV-aPDS, and WMV-hPDS exhibited a photobleaching phenotype compatible with *PDS* silencing (Fig. 2). Three weeks after inoculation, leaf samples were taken for RNA analyses. Reverse transcription (RT)-polymerase chain reaction (PCR) amplification of the viral CP cistron, followed by electrophoretic analysis of the products, confirmed the presence of the virus in all agroinoculated plants, except for those mock-inoculated (Fig. 3A). RT-PCR analysis encompassing the NIb/CP intercistronic site, in which the exogenous cDNA was inserted, indicated that, while the sense and antisense *PDS* fragments were stable in the viral progeny,

the hairpin was lost (Fig. 3B). Sequence analysis of the progenies accumulating in plants infected by WMV-hPDS indicated nearly full deletion of the inserted sequences in the progeny, as a consequence of different recombination events. One of these events is outlined, as an example, in Fig. 4. Finally, RT-quantitative PCR (qPCR) analysis of *PDS* mRNA at 28 dpi confirmed gene silencing in systemic tissues of plants infected with WMV-sPDS, WMV-aPDS, and WMV-hPDS, in contrast to those mock-inoculated or infected with WMV-Vera (Fig. 5A). These results indicate that the Vera isolate of WMV can be used as a vector for gene function analyses in melon.

To confirm these results, we targeted another melon gene using the WMV VIGS vector. We chose *Magnesium chelatase subunit I* (*CHLI*). Magnesium chelatase is a three-component enzyme (CHLI, CHLD, and CHLH) that catalyzes the insertion of Mg^{2+} into protoporphyrin IX, in the first committed and key regulatory step of chlorophyll biosynthesis (Stenbaek and Jensen 2010). Silencing of *CHLI* can be easily tracked by a foliar decoloration phenotype, as a consequence of deficient chlorophyll accumulation. Since we previously obtained significant silencing in all three assayed modalities (sense, antisense, and hairpin) (Fig. 5A), we built the VIGS vector pGWMV-sCHLI (Supplementary Fig. S1) to express the *CHLI* ORF 5' 201 nt only in a sense orientation. The melon plants were agroinoculated with *A. tumefaciens* bearing the empty plasmid pG35Z, pGWMV-Vera, or pGWMV-sCHLI. Again, two weeks after inoculation, we detected symptoms of infection in plants inoculated with the wild-type virus and WMV-sCHLI. Interestingly, systemic tissues of plants infected with this second virus exhibited decolored spots, suggesting *CHLI* silencing (Fig. 6A). RT-qPCR analysis of RNA preparations from systemic leaf samples from these plants at 28 dpi confirmed the presence of the inserted fragment of exogenous RNA in the viral progeny (Fig. 6B), indicating *CHLI* silencing (Fig. 5B).

Construction of a WMV-based VIGS vector for easy cloning

Finally, to facilitate the use of this novel VIGS vector among the research community interested in cucurbit gene function analysis, we built a new binary plasmid containing the full-length WMV-Vera infectious clone, with the rearranged artificial NIaPro cleavage site between NIb and CP and with a unique *Mlu*I cleavage site to facilitate plasmid linearization and the insertion of the foreign gene fragment in a single Gibson assembly step. This plasmid, named pGWMV-VIGS (Supplementary Fig. S1), was deposited in Addgene (accession number pending).

Discussion

Our results show that an infectious clone of a mild isolate of WMV (Aragonés et al. 2019) can be used as a VIGS vector to study gene function in melon. This new system adds to those previously reported for VIGS in melon and other cucurbits, based on *Apple latent spherical virus* (ALSV, genus *Cheravirus*, family *Secoviridae*) (Igarashi et al. 2009), *Tobacco rattle virus* (TRV, genus *Tobravirus*, family *Virgaviridae*) (Zhao et al. 2016), and—in particular—*Cucumber green mottle mosaic virus* (CGMMV; genus *Tobamovirus*, family *Virgaviridae*). The latter has been recently shown to induce a long-lasting silencing of *PDS* in watermelon, melon, cucumber, and bottle gourd (Liu et al. 2020). Although we have only performed experiments on melon, because WMV presents a broad host range—160 dicotyledonous species of 23 families (Desbiez and Lecoq 2004; Ouibrahim et al. 2014; Peláez et al. 2020)—we expect this new system to be useful in other cucurbits, as well as species outside this family that also host the virus. The vector is based on a single binary plasmid carrying kanamycin resistance, as well as two origins of replication in *E. coli* and *A. tumefaciens*. The exogenous sequence fragment homologous to the gene selected for silencing can be inserted between the two parts of a rearranged artificial NIaPro cleavage site at the NIb/CP intercistronic position, after a simple *Mlu*I digestion of the vector and an assembly reaction (Gibson et al. 2009). The two parts of the artificial NIaPro cleavage site complement the split NIb/CP cleavage site, facilitating NIb/heterologous protein and heterologous protein/CP proteolytic cleavages (Fig. 1). In this way, the translation product corresponding to the exogenous sequence is efficiently released from the viral polyprotein, likely reducing the impact on virus viability. However, the exogenous sequence must be inserted in a way that does not change the reading frame of the large viral polyprotein. The plasmid vector, named pGWMV-VIGS, has been deposited in Addgene (accession number pending) to facilitate exchange and to promote its use by the research community interested in cucurbit genetics. Because pGWMV-VIGS ultimately derives from pCLEAN-G181 (Aragonés et al. 2019), this plasmid requires a pSOUP-series helper for replication in *A. tumefaciens* (Thole et al. 2007).

WMV belongs to the genus *Potyvirus*, the largest group of RNA viruses that infect plants (Revers and García 2015; Wylie et al. 2017). Relatively few VIGS vectors have been derived to date from this large group of viruses, whose diversity remains mostly underutilized for reverse genetic analyses. This is likely a consequence of the strong RNA silencing suppressor activity of potyviral HC-Pro (Kasschau and Carrington 1998; Valli et al. 2018),

339 which is reinforced by that of the viral protein genome-linked (VPg) (Rajamäki and Valkonen
340 2009). The combined activities of HC-Pro and VPg efficiently cancel the host RNA-based
341 antiviral response. For this reason, viruses with weak and mild RNA silencing suppressors are
342 typically preferred as VIGS vectors (Baulcombe 1999). Our results demonstrate that particular
343 potyvirus isolates—such as WMV-Vera (Aragonés et al. 2019)—which induce mild symptoms
344 and, presumably, must harbor mild silencing suppressors, can be used as vectors for efficient
345 VIGS. In addition to exploring natural variation, potyvirus infectious clones may also be
346 mutagenized to reduce the activity of their RNA silencing suppressors, in order to be used as
347 efficient VIGS vectors (Torres-Barceló et al. 2008, 2010; Wu et al. 2010).
348 The second constraint of potyviruses as vectors for VIGS is their particular genome
349 organization, which contains an almost genome-long polyprotein (Revers and García 2015). It
350 is unlikely that the exogenous sequences can be inserted in the viral 5' or 3' UTRs without
351 dramatically affecting virus infectivity. Potyvirus 5' UTRs are highly structured and contain
352 cap-independent regulatory translation elements (Niepel and Gallie 1999; Zeenko and Gallie
353 2005). 3' UTRs, together with the final part of CP cistrons, fold in a complex secondary
354 structure involved in viral genome amplification (Haldeman-Cahill et al. 1998). As an
355 alternative, the exogenous gene fragment can be inserted into an intercistronic position. An NIb
356 relocation analysis showed that the only permitted intercistronic positions in *Tobacco etch virus*
357 (TEV; genus *Potyvirus*) were in front of P1, P1/HC-Pro, and NIb/CP. NIb insertion in the other
358 intercistronic positions generated non-viable viruses (Majer et al. 2014). However, a different
359 study using *Turnip mosaic virus* (TuMV; genus *Potyvirus*) reported tolerance to inserting
360 foreign sequences also at HC-Pro/P3, 6K1/CI, and NIaPro/NIb intercistronic sites (Chen et al.
361 2007). In our experiments, we exclusively explored the NIb/CP intercistronic site, which is a
362 classic position for inserting heterologous sequences in potyvirus-based vectors (Choi et al.
363 2000), although other positions may be equally well-suited.
364 To gain insight into potyvirus-based VIGS, we explored the silencing efficiency and
365 vector stability that resulted from expressing exogenous sequences under different modalities:
366 sense, antisense, and hairpin. All three constructs produced a significant reduction of the *PDS*
367 mRNA (Fig. 5A). Although the antisense modality had the largest effect on average, the
368 differences were not statistically significant. However, while the sense and antisense constructs
369 remained stable in the viral progeny, the hairpin was rapidly lost (Fig. 3B and Fig. 4).
370 Remarkably, it still triggered a gene silencing effect of the same intensity as the sense and
371 antisense counterparts that remained in the progeny (Fig. 5A). This indicates that, once
372 unleashed, the plant silencing machinery amplifies and transitorily maintains the silencing

signal in the absence of the trigger. Since no significant differences were observed between the sense, antisense, and hairpin constructs, we preferred the sense modality for further assays (Fig. 5B) because maintaining the viral ORF is straightforward in this case.

In our hairpin construct, we used a group-I self-splicing intron from the rRNA of *T. thermophila* as an alternative to a plant intron processed by the spliceosome, which is typically used to express hairpin constructs in plants (Smith et al. 2000). Efficient self-splicing of the *T. thermophila* group-I intron is indicated by the high infectivity of WMV-hPDS, comparable to that of WMV-sPDS and WMV-aPDS (Fig. 3A). Some spliceosomal introns—typically intron-2 from the *Piruvate orthophosphate dikinase* (*Pdk*) gene of *Flaveria trinervia* (Rosche and Westhoff 1995; Smith et al. 2000)—are frequently used to express hairpin constructs in plants and have demonstrated broad functionality in many plant species. Nevertheless, we believe that a self-splicing intron, such as that used in our study, must be universally applied because it only requires a guanosine nucleoside for processing (Zaug and Cech 1986). In this way, the use of this self-splicing intron allows the correct formation of the hairpin motif—not only in plants but also in species belonging to other domains (Ortolá et al. 2021). This technique can even be applied *in vitro* if more complex experimental strategies require it.

In conclusion, we have developed a new VIGS vector, based on a mild isolate of WMV, that we expect to be useful in reverse genetics analyses particularly in melon and other cucurbits. In addition, we contribute new techniques, such as the use of mild isolates and the insertion of in-frame sense fragments of the exogenous genes, which may facilitate the incorporation of many more potyviruses into VIGS technology.

Acknowledgements. This research was supported by grants BIO2017-83184-R, AGL2017-85563-C2-1-R and RTA2017-00061-C03-03 from Ministerio de Ciencia e Innovación (Spain), through Agencia Estatal de Investigación (cofinanced European Regional Development Fund).

Author contribution statements. B.P. C.L. and J-A.D. designed the project. F.H., V.A., A.B. and C.S. performed the experiments. All authors analyzed the data. J-A.D. wrote the manuscript with input from all the authors.

Compliance with ethical standards

Conflict of interest. The authors declare that they have no conflict of interest.

References

Aragonés V, Pérez-de-Castro A, Cordero T, Cebolla-Cornejo J, López C, Picó B, Daròs JA (2019) A Watermelon mosaic virus clone tagged with the yellow visual maker phytoene synthase facilitates scoring infectivity in melon breeding programs. Eur J Plant Pathol 153:317–323

Baulcombe DC (1999) Fast forward genetics based on virus-induced gene silencing. Curr Opin Plant Biol 2:109–113

Bertin S, Manglli A, McLeish M, Tomassoli L (2020) Genetic variability of watermelon mosaic virus isolates infecting cucurbit crops in Italy. Arch Virol 165:937–946

Burch-Smith TM, Schiff M, Liu Y, Dinesh-Kumar SP (2006) Efficient virus-induced gene silencing in Arabidopsis. Plant Physiol 142:21–7

Chen CC, Chen TC, Raja JA, Chang CA, Chen LW, Lin SS, Yeh SD (2007) Effectiveness and stability of heterologous proteins expressed in plants by Turnip mosaic virus vector at five different insertion sites. Virus Res 130:210–227

Choi IR, Stenger DC, Morris TJ, French R (2000) A plant virus vector for systemic expression of foreign genes in cereals. Plant J 23:547–555

Chomicki G, Schaefer H, Renner SS (2020) Origin and domestication of Cucurbitaceae crops: insights from phylogenies, genomics and archaeology. New Phytol. 226:1240–1255

Cordero T, Cerdan L, Carbonell A, Katsarou K, Kalantidis K, Daròs JA (2017) Dicer-like 4 is involved in restricting the systemic movement of zucchini yellow mosaic virus in nicotiana benthamiana. Mol Plant-Microbe Interact 30:63–71

Courdavault V, Besseau S, Oudin A, Papon N, O'Connor SE (2020) Virus-Induced Gene Silencing: Hush Genes to Make Them Talk. Trends Plant Sci. 25:714–715

Csorba T, Kontra L, Burgyàn J (2015) Viral silencing suppressors: tools forged to fine-tune host-pathogen coexistence. Virology 479–480:85–103

Desbiez C, Lecoq H (2004) The nucleotide sequence of Watermelon mosaic virus (WMV, Potyvirus) reveals interspecific recombination between two related potyviruses in the 5' part of the genome. Arch Virol 149:1619–1632

Desbiez C, Wipf-Scheibel C, Millot P, Berthier K, Girardot G, Gognalons P, Hirsch J, Moury B, Nozeran K, Piry S, Schoeny A, Verdin E (2020) Distribution and evolution of the major viruses infecting cucurbitaceous and solanaceous crops in the French Mediterranean area. Virus Res 286:198042

Dommes AB, Gross T, Herbert DB, Kivivirta KI, Becker A (2019) Virus-induced gene

441 silencing: Empowering genetics in non-model organisms. J Exp Bot 70:817–833
442 Fofana IBF, Sangaré A, Collier R, Taylor C, Fauquet CM (2004) A geminivirus-induced gene
443 silencing system for gene function validation in cassava. Plant Mol Biol 56:613–624
444 Gammelgård E, Mohan M, Valkonen JPT (2007) Potyvirus-induced gene silencing: The
445 dynamic process of systemic silencing and silencing suppression. J Gen Virol 88:2337–
446 2346
447 Gibson DG, Young L, Chuang RY, Venter JC, Hutchison 3rd CA, Smith HO (2009)
448 Enzymatic assembly of DNA molecules up to several hundred kilobases. Nat Methods
449 6:343–345
450 Gonzalez-Ibeas D, Blanca J, Roig C, González-To M, Picó B, Truniger V, Gómez P, Deleu
451 W, Caño-Delgado A, Arús P, Nuez F, Garcia-Mas J, Puigdomènech P, Aranda MA
452 (2007) MELOGEN: An EST database for melon functional genomics. BMC Genomics
453 8:306
454 Haldeman-Cahill R, Daròs J-A, Carrington JC (1998) Secondary Structures in the Capsid
455 Protein Coding Sequence and 3′ Nontranslated Region Involved in Amplification of the
456 Tobacco Etch Virus Genome. J Virol 72:4072–4079
457 Holzberg S, Brosio P, Gross C, Pogue GP (2002) Barley stripe mosaic virus-induced gene
458 silencing in a monocot plant. Plant J 30:315–327
459 Igarashi A, Yamagata K, Sugai T, Takahashi Y, Sugawara E, Tamura A, Yaegashi H,
460 Yamagishi N, Takahashi T, Isogai M, Takahashi H, Yoshikawa N (2009) Apple latent
461 spherical virus vectors for reliable and effective virus-induced gene silencing among a
462 broad range of plants including tobacco, tomato, Arabidopsis thaliana, cucurbits, and
463 legumes. Virology 386:407–416
464 Jones AL, Thomas CL, Maule AJ (1998) De novo methylation and co-suppression induced by
465 a cytoplasmically replicating plant RNA virus. EMBO J 17:6385–6393
466 Kant R, Dasgupta I (2019) Gene silencing approaches through virus-based vectors: speeding
467 up functional genomics in monocots. Plant Mol. Biol. 100:3–18
468 Kasschau KD, Carrington JC (1998) A counterdefensive strategy of plant viruses: suppression
469 of posttranscriptional gene silencing. Cell 95:461–470
470 Kjemtrup S, Sampson KS, Peele CG, Nguyen L V., Conkling MA, Thompson WF, Robertson
471 D (1998) Gene silencing from plant DNA carried by a Geminivirus. Plant J 14:91–100
472 Kumagai MH, Donson J, della-Cioppa G, Harvey D, Hanley K, Grill LK (1995) Cytoplasmic
473 inhibition of carotenoid biosynthesis with virus-derived RNA. Proc Natl Acad Sci USA
474 92:1679–1683

475 Lai PJ, Lim CT, Le HP, Katayama T, Leach DRF, Furukohri A, Maki H (2016) Long inverted
476 repeat transiently stalls DNA replication by forming hairpin structures on both leading
477 and lagging strands. Genes to Cells 21:136–145
478 Lindbo JA, Silva-Rosales L, Proebsting WM, Dougherty WG (1993) Induction of a highly
479 specific antiviral state in transgenic plants: Implications for regulation of gene
480 expression and virus resistance. Plant Cell 5:1749–1759
481 Liu M, Liang Z, Aranda MA, Hong N, Liu L, Kang B, Gu Q (2020) A cucumber green mottle
482 mosaic virus vector for virus-induced gene silencing in cucurbit plants. Plant Methods
483 16:9
484 Liu Y, Schiff M, Dinesh-Kumar SP (2002a) Virus-induced gene silencing in tomato. Plant J
485 31:777–786
486 Liu Y, Schiff M, Marathe R, Dinesh-Kumar SP (2002b) Tobacco Rar1, EDS1 and
487 NPR1/NIM1 like genes are required for N-mediated resistance to tobacco mosaic virus.
488 Plant J 30:415–429
489 Livak KJ, Schmittgen TD (2001) Analysis of relative gene expression data using real-time
490 quantitative PCR and the 2-ΔΔCT method. Methods 25:402–408
491 Majer E, Salvador Z, Zwart MP, Willemsen A, Elena SF, Daros J-A (2014) Relocation of the
492 NIb Gene in the Tobacco Etch Potyvirus Genome. J Virol 88:4586–4590
493 Niepel M, Gallie DR (1999) Identification and characterization of the functional elements
494 within the tobacco etch virus 5' leader required for cap-independent translation. J Virol
495 73:9080–9088
496 Olspert A, Carr JP, Firth AE (2016) Mutational analysis of the Potyviridae transcriptional
497 slippage site utilized for expression of the P3N-PIPO and P1N-PISPO proteins. Nucleic
498 Acids Res 44:7618–7629
499 Ortolá B, Cordero T, Hu X, Daròs J-A (2021) Intron-assisted, viroid-based production of
500 insecticidal circular double-stranded RNA in Escherichia coli. RNA Biol.
501 https://doi.org/10.1080/15476286.2021.1872962
502 Ouibrahim L, Mazier M, Estevan J, Pagny G, Decroocq V, Desbiez C, Moretti A, Gallois JL,
503 Caranta C (2014) Cloning of the Arabidopsisrwm1 gene for resistance to Watermelon
504 mosaic virus points to a new function for natural virus resistance genes. Plant J 79:705–
505 716
506 Peláez A, McLeish MJ, Paswan RR, Dubay B, Fraile A, García-Arenal F (2020) Ecological
507 fitting is the forerunner to diversification in a plant virus with broad host range. J Evol
508 Biol jeb.13672

509 Rajamäki ML, Valkonen JP (2009) Control of nuclear and nucleolar localization of nuclear
510 inclusion protein a of picorna-like Potato virus A in Nicotiana species. Plant Cell
511 21:2485–2502
512 Revers F, García JA (2015) Molecular biology of potyviruses. Adv Virus Res 92:101–199
513 Rosche E, Westhoff P (1995) Genomic structure and expression of the pyruvate,
514 orthophosphate dikinase gene of the dicotyledonous C4 plant Flaveria trinervia
515 (Asteraceae). Plant Mol Biol 29:663–678
516 Smith NA, Singh SP, Wang MB, Stoutjesdijk PA, Green AG, Waterhouse PM (2000) Total
517 silencing by intron-spliced hairpin RNAs. Nature 407:319–320
518 Stenbaek A, Jensen PE (2010) Redox regulation of chlorophyll biosynthesis. Phytochemistry
519 71:853–859
520 Teresa Ruiz M, Voinnet O, Baulcombe DC (1998) Initiation and maintenance of virus-
521 induced gene silencing. Plant Cell 10:937–946
522 Thole V, Worland B, Snape JW, Vain P (2007) The pCLEAN dual binary vector system for
523 Agrobacterium-mediated plant transformation. Plant Physiol 145:1211–1219
524 Torres-Barceló C, Daròs JA, Elena SF (2010) HC-Pro hypo- and hypersuppressor mutants:
525 Differences in viral siRNA accumulation in vivo and siRNA binding activity in vitro.
526 Arch Virol 155:251–254
527 Torres-Barceló C, Martín S, Daròs JA, Elena SF (2008) From hypo- to hypersuppression:
528 Effect of amino acid substitutions on the RNA-silencing suppressor activity of the
529 Tobacco etch potyvirus HC-pro. Genetics 180:1039–1049
530 Valli AA, Gallo A, Rodamilans B, Lopez-Moya JJ, Garcia JA (2018) The HCPro from the
531 Potyviridae family: an enviable multitasking Helper Component that every virus would
532 like to have. Mol Plant Pathol 19:744–763
533 Weng Y, Garcia-Mas J, Levi A, Luan F (2020) Editorial: Translational Research for Cucurbit
534 Molecular Breeding: Traits, Markers, and Genes. Front Plant Sci 11:615346
535 Wu HW, Lin SS, Chen KC, Yeh SD, Chua NH (2010) Discriminating mutations of HC-Pro of
536 Zucchini yellow mosaic virus with differential effects on small RNA pathways involved
537 in viral pathogenicity and symptom development. Mol Plant-Microbe Interact 23:17–28
538 Wylie SJ, Adams M, Chalam C, Kreuze J, López-Moya JJ, Ohshima K, Praveen S,
539 Rabenstein F, Stenger D, Wang A, Zerbini FM, Ictv Report C, Lopez-Moya JJ, Ohshima
540 K, Praveen S, Rabenstein F, Stenger D, Wang A, Murilo Zerbini F, Ictv Report C (2017)
541 ICTV Virus Taxonomy Profile: Potyviridae. J Gen Virol 98:352–354
542 Zaug AJ, Cech TR (1986) The intervening sequence RNA of Tetrahymena is an enzyme.

543 Science (80-) 231:470–475
544 Zeenko V, Gallie DR (2005) Cap-independent translation of tobacco etch virus is conferred
545 by an RNA pseudoknot in the 5′-leader. J Biol Chem 280:26813–26824
546 Zhao F, Lim S, Igori D, Yoo RH, Kwon SY, Moon JS (2016) Development of tobacco
547 ringspot virus-based vectors for foreign gene expression and virus-induced gene
548 silencing in a variety of plants. Virology 492:166–178
549

Figures

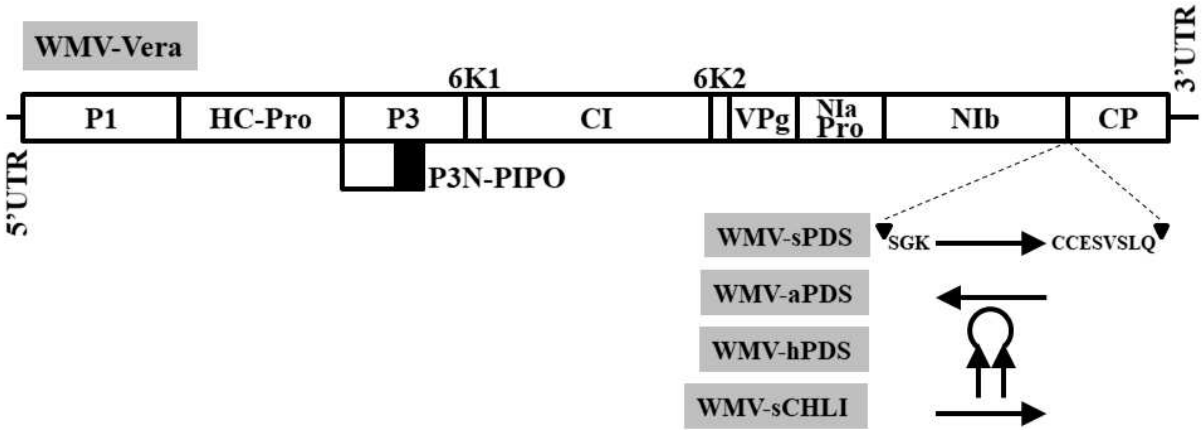

Fig. 1. Schematic representation of the WMV genome. Lines and boxes represent the 5' and 3' UTRs and protein-coding cistrons, as indicated. In pMWMV-Z and pGMWV-VIGS, an artificial NIaPro cleavage site was inserted at the NIb/CP intercistronic site. The amino acid sequence is indicated. The exogenous sequences inserted in WMV-sPDS, WMV-aPDS, WMV-hPDS, and WMV-sCHLI are also schematically represented.

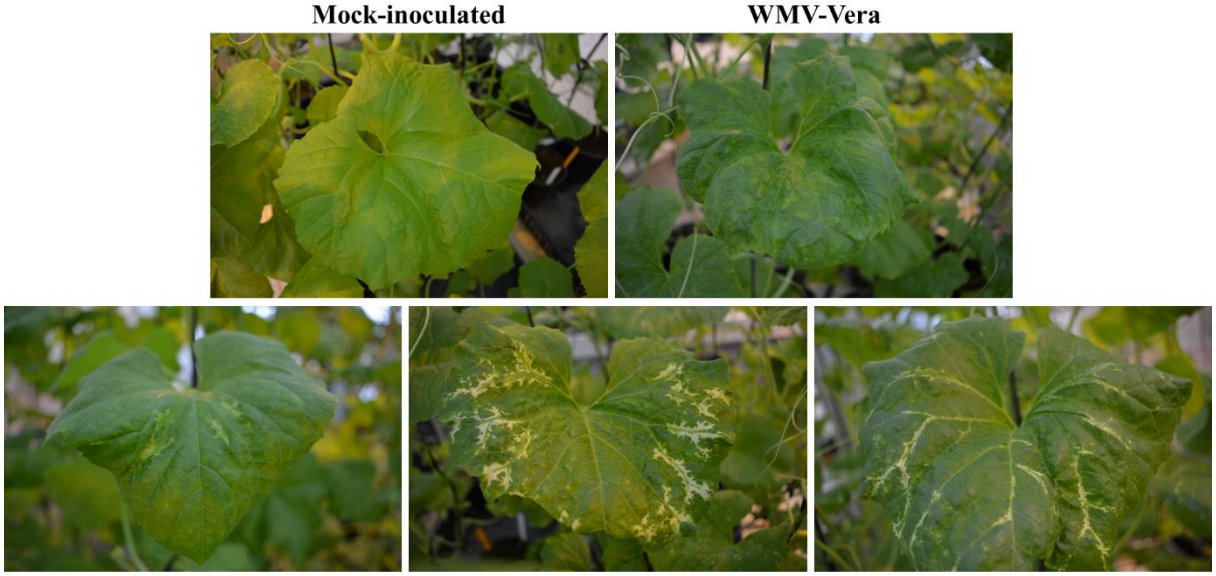

559

560

561 **Fig. 2.** Photographs of representative leaves of melon plants mock-inoculated or inoculated
562 with WMV-Vera, WMV-sPDS, WMV-aPDS, or WMV-hPDS, as indicated. Leaves correspond
563 to systemic non-inoculated leaves; the photographs were taken at 28 dpi.

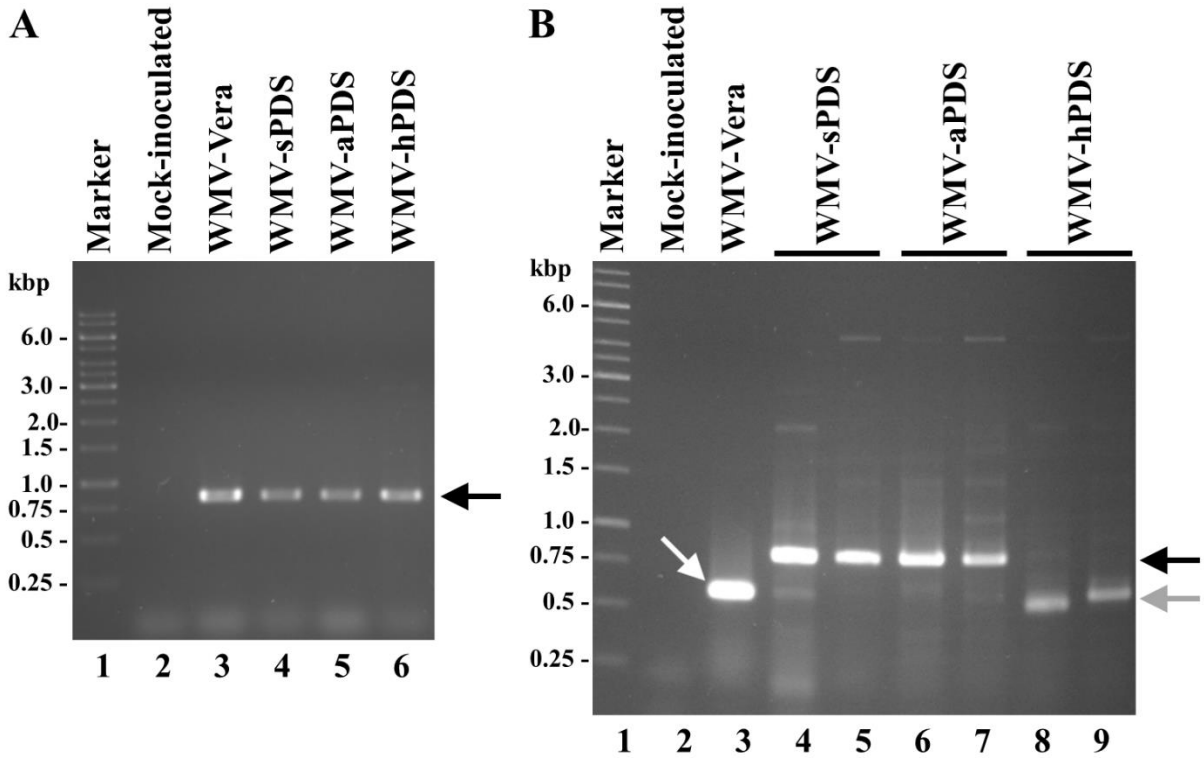

564

565

566 **Fig. 3.** RT-PCR analysis of the viral progeny. (**A**) Infection diagnosis by RT-PCR amplification
567 of the CP cistron 15 dpi. (**B**) RT-PCR analysis of the inserted exogenous sequence 21 dpi. RNA
568 preparations from systemic non-inoculated leaves were subjected to RT-PCR amplification; the
569 products were separated by electrophoreses in agarose gels that were stained with ethidium
570 bromide. (**A** and **B**) Lanes 1, DNA marker with the sizes (in kbp) of some of the standards on
571 the left; lanes 2 and 3, single representative plants mock-inoculated and inoculated with WMV-
572 Vera, respectively. (**A**) Lanes 4 to 6, single representative plants inoculated with WMV-sPDS,
573 WMV-aPDS, and WMV-hPDS, respectively. Black arrow points to the WMV CP cistron
574 cDNA product. (**B**) Lanes 4 to 9, two representative plants inoculated with WMV-sPDS (lanes
575 4 and 5), WMV-aPDS (lanes 6 and 7), and WMV-hPDS (lanes 8 and 9). White, black, and gray
576 arrows point to cDNA products with no exogenous sequence, those that maintained the
577 sequence, and those that lost the sequence, respectively.

578

579

580 **Fig. 4.** Consensus sequence at the NIb/CP intercistronic site in the progeny of a representative
581 plant infected with WMV-hPDS. RNA was purified from upper non-inoculated leaves at 21 dpi
582 and subjected to RT-PCR amplification. The amplification product was purified and sequenced.

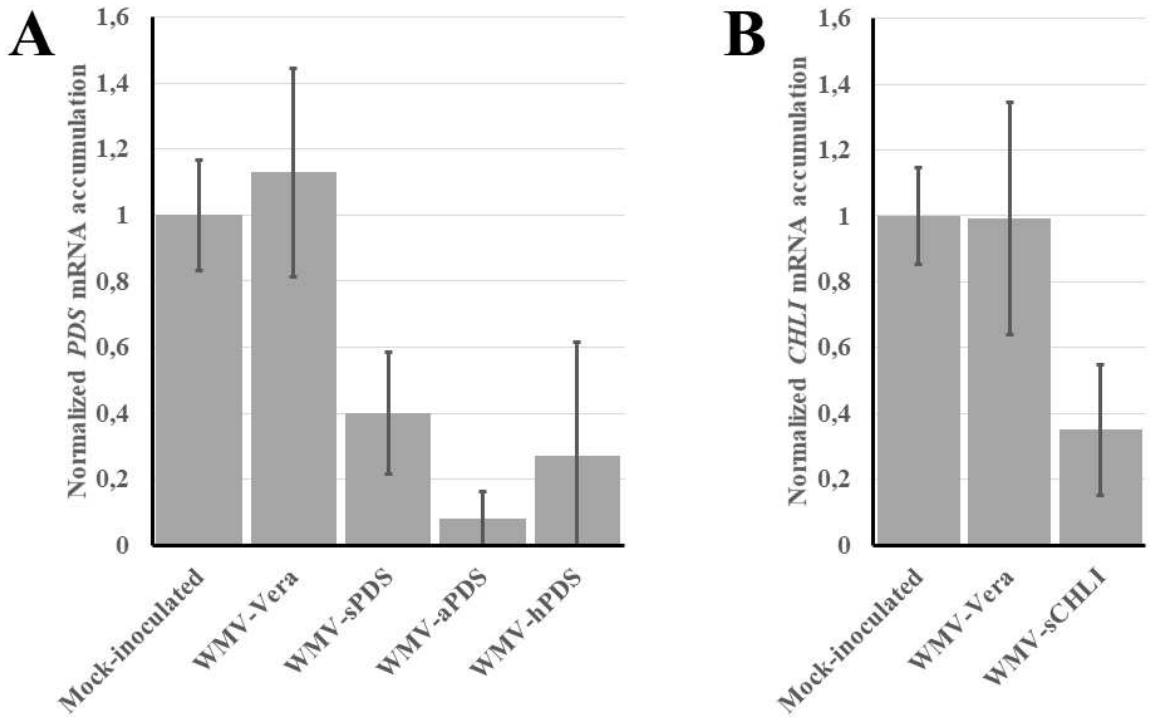

583

584

585 **Fig. 5.** RT-qPCR analysis of (**A**) *PDS* and (**B**) *CHLI* mRNAs. Columns represent the
586 normalized average mRNA accumulation in three independent plants (two technical replicates
587 per plant). The average *PDS* and *CHLI* mRNA accumulations in the mock-inoculated plants
588 were used for normalization in (**A**) and (**B**), respectively.

589

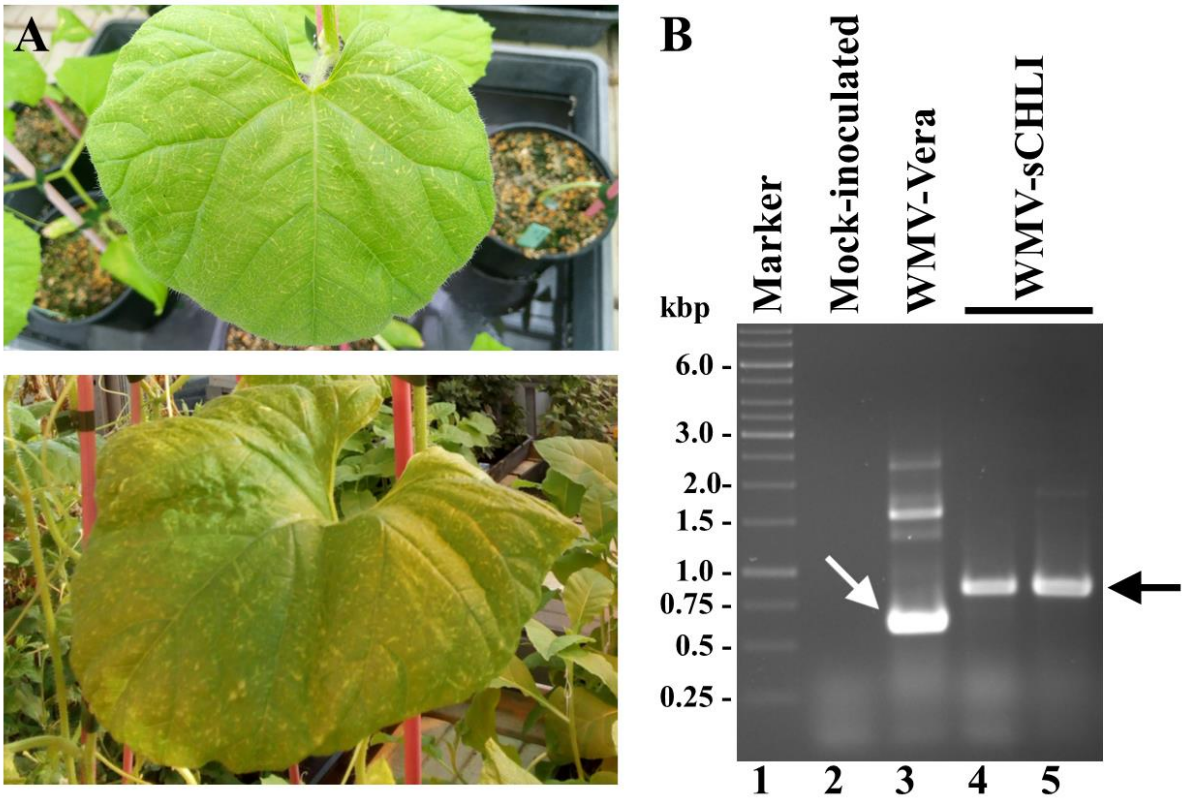

590
591

592 **Fig. 6.** Analyses of melon plants inoculated with WMV-sCHLI. (**A**) Photographs were taken at
593 28 dpi of representative plants agroinoculated with WMV-sCHLI. (**B**) RT-PCR analysis of the
594 inserted exogenous sequence at 21 dpi, as indicated in the legend for Fig. 3B. Lane 1, DNA
595 marker with the sizes (in kbp) of some of the standards on the left; lanes 2 and 3, single
596 representative plants mock-inoculated and inoculated with WMV-Vera; lanes 4 and 5, two
597 representative plants inoculated with WMV-sCHLI.

Figures

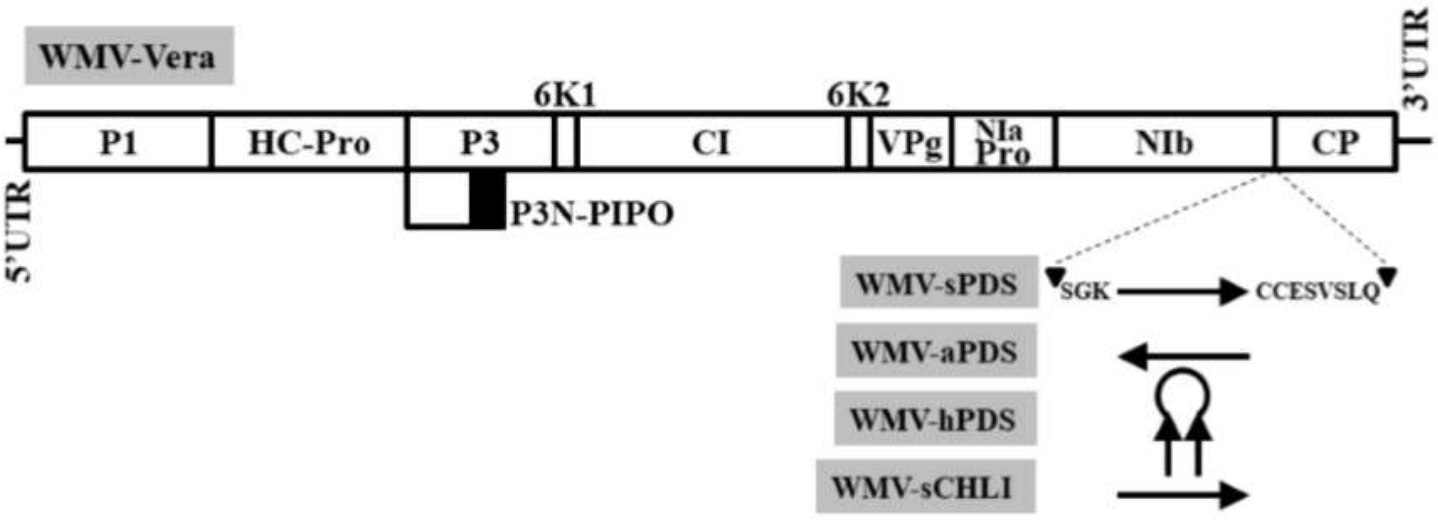

Figure 1

Schematic representation of the WMV genome. Lines and boxes represent the 5' and 3' UTRs and protein-coding cistrons, as indicated. In pMWMV-Z and pGMWV-VIGS, an artificial NIaPro cleavage site was inserted at the NIb/CP intercistronic site. The amino acid sequence is indicated. The exogenous sequences inserted in WMV-sPDS, WMV-aPDS, WMV- hPDS, and WMV-sCHLI are also schematically represented.

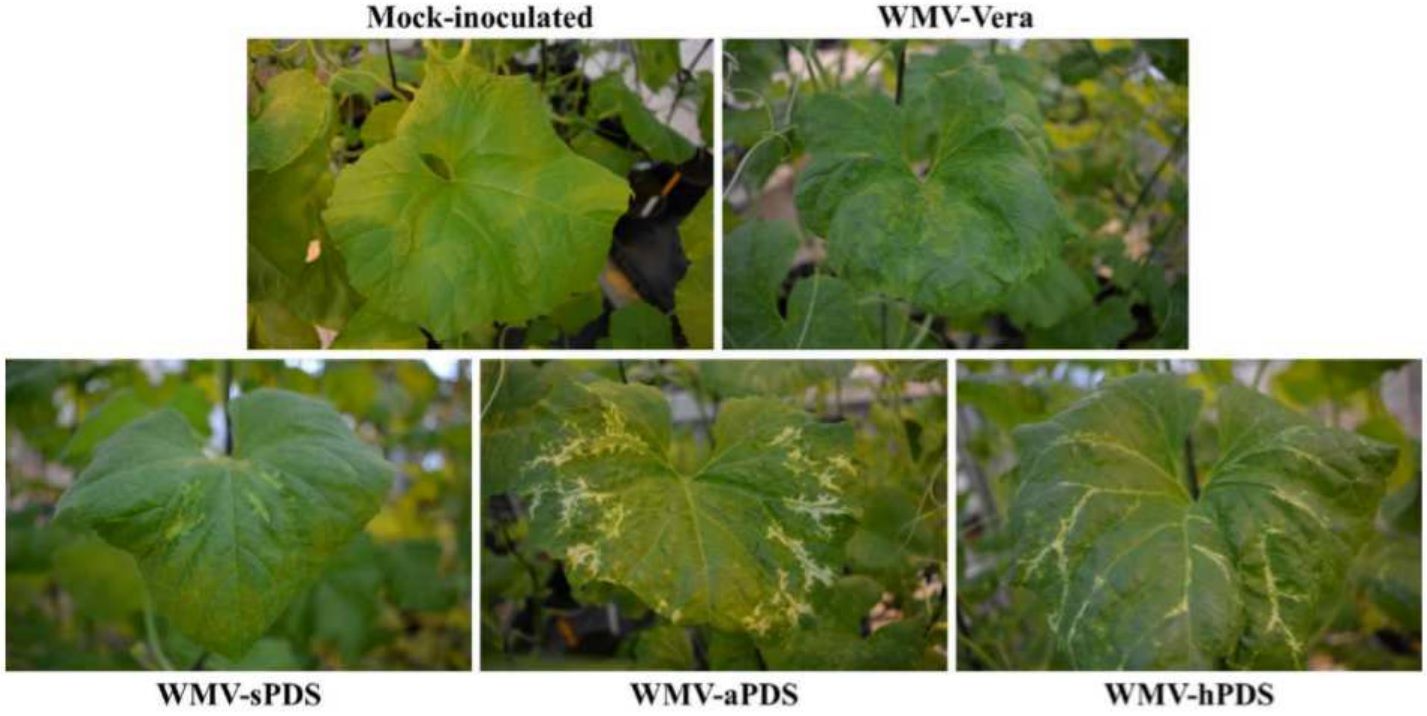

Figure 2

Photographs of representative leaves of melon plants mock-inoculated or inoculated with WMV-Vera, WMV-sPDS, WMV-aPDS, or WMV-hPDS, as indicated. Leaves correspond to systemic non-inoculated leaves; the photographs were taken at 28 dpi.

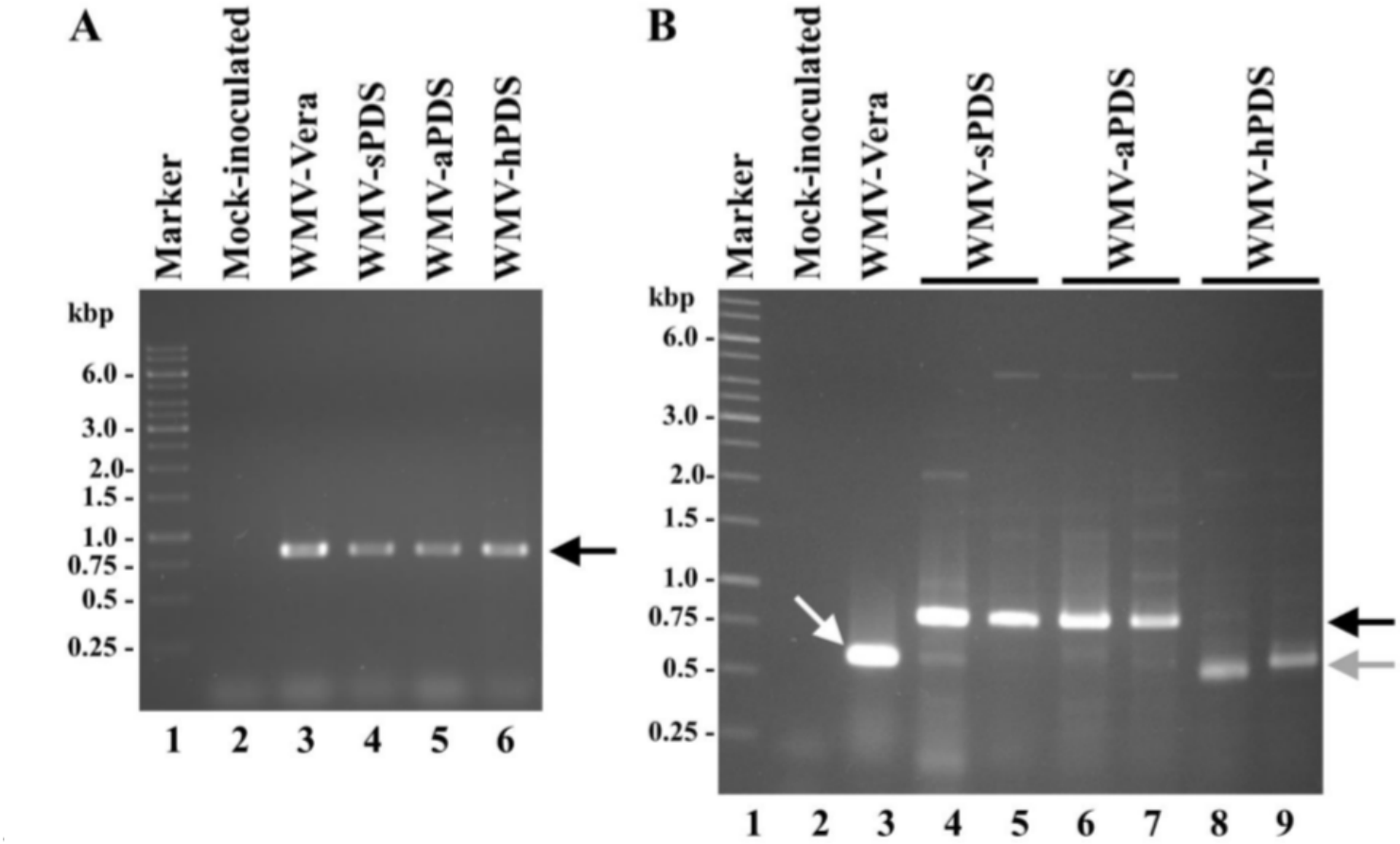

Figure 3

RT-PCR analysis of the viral progeny. (A) Infection diagnosis by RT-PCR amplification of the CP cistron 15 dpi. (B) RT-PCR analysis of the inserted exogenous sequence 21 dpi. RNA preparations from systemic non-inoculated leaves were subjected to RT-PCR amplification; the products were separated by electrophoreses in agarose gels that were stained with ethidium bromide. (A and B) Lanes 1, DNA marker with the sizes (in kbp) of some of the standards on the left; lanes 2 and 3, single representative plants mock-inoculated and inoculated with WMV- Vera, respectively. (A) Lanes 4 to 6, single representative plants inoculated with WMV-sPDS, WMV-aPDS, and WMV-hPDS, respectively. Black arrow points to the WMV CP cistron cDNA product. (B) Lanes 4 to 9, two representative plants inoculated with WMV-sPDS (lanes 4 and 5), WMV-aPDS (lanes 6 and 7), and WMV-hPDS (lanes 8 and 9). White, black, and gray arrows point to cDNA products with no exogenous sequence, those that maintained the sequence, and those that lost the sequence, respectively.

Figure 4

Consensus sequence at the NIb/CP intercistronic site in the progeny of a representative plant infected with WMV-hPDS. RNA was purified from upper non-inoculated leaves at 21 dpi and subjected to RT-PCR amplification. The amplification product was purified and sequenced.

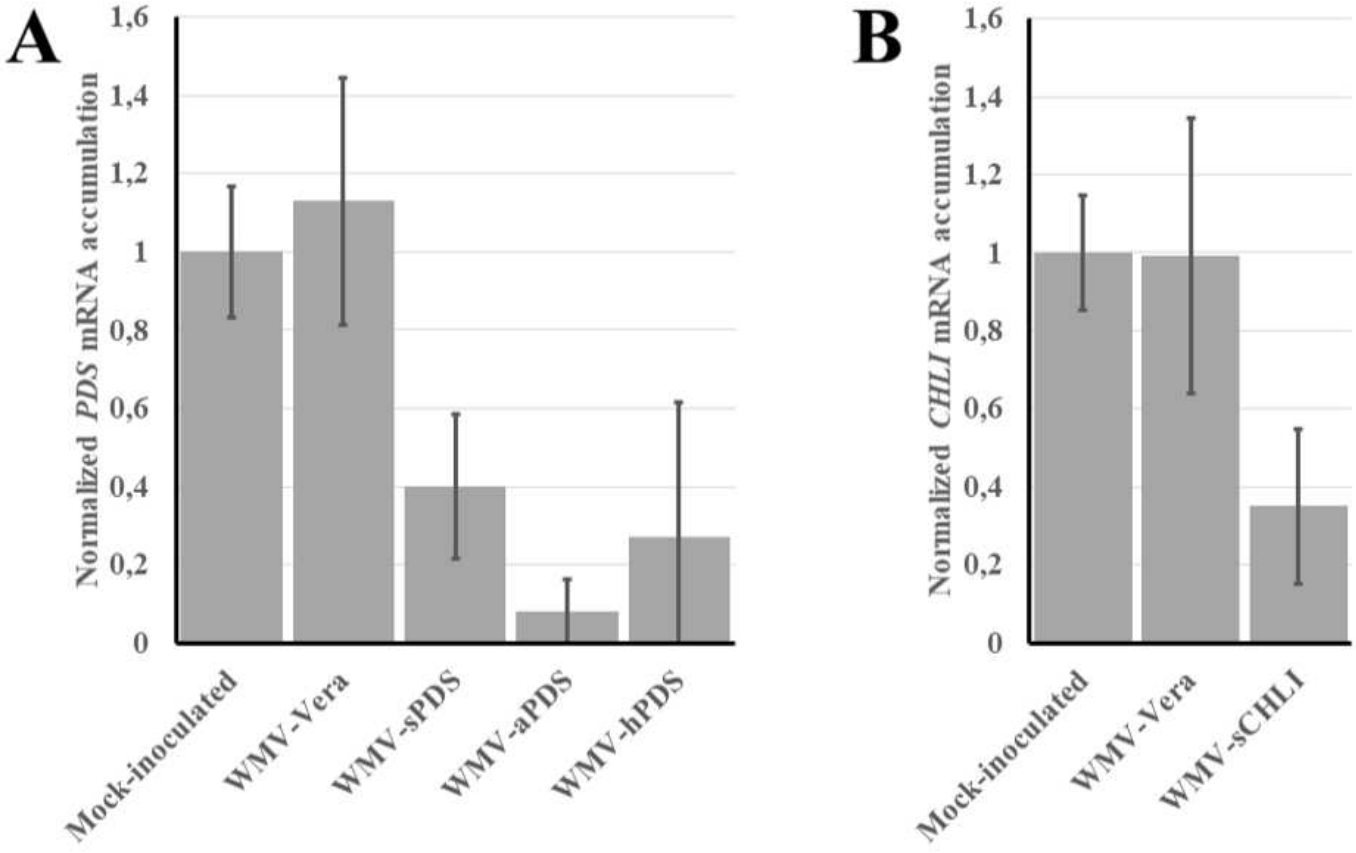

Figure 5

RT-qPCR analysis of (A) PDS and (B) CHLI mRNAs. Columns represent the 585 normalized average mRNA accumulation in three independent plants (two technical replicates per plant). The average PDS and CHLI mRNA accumulations in the mock-inoculated plants were used for normalization in (A) and (B), respectively.

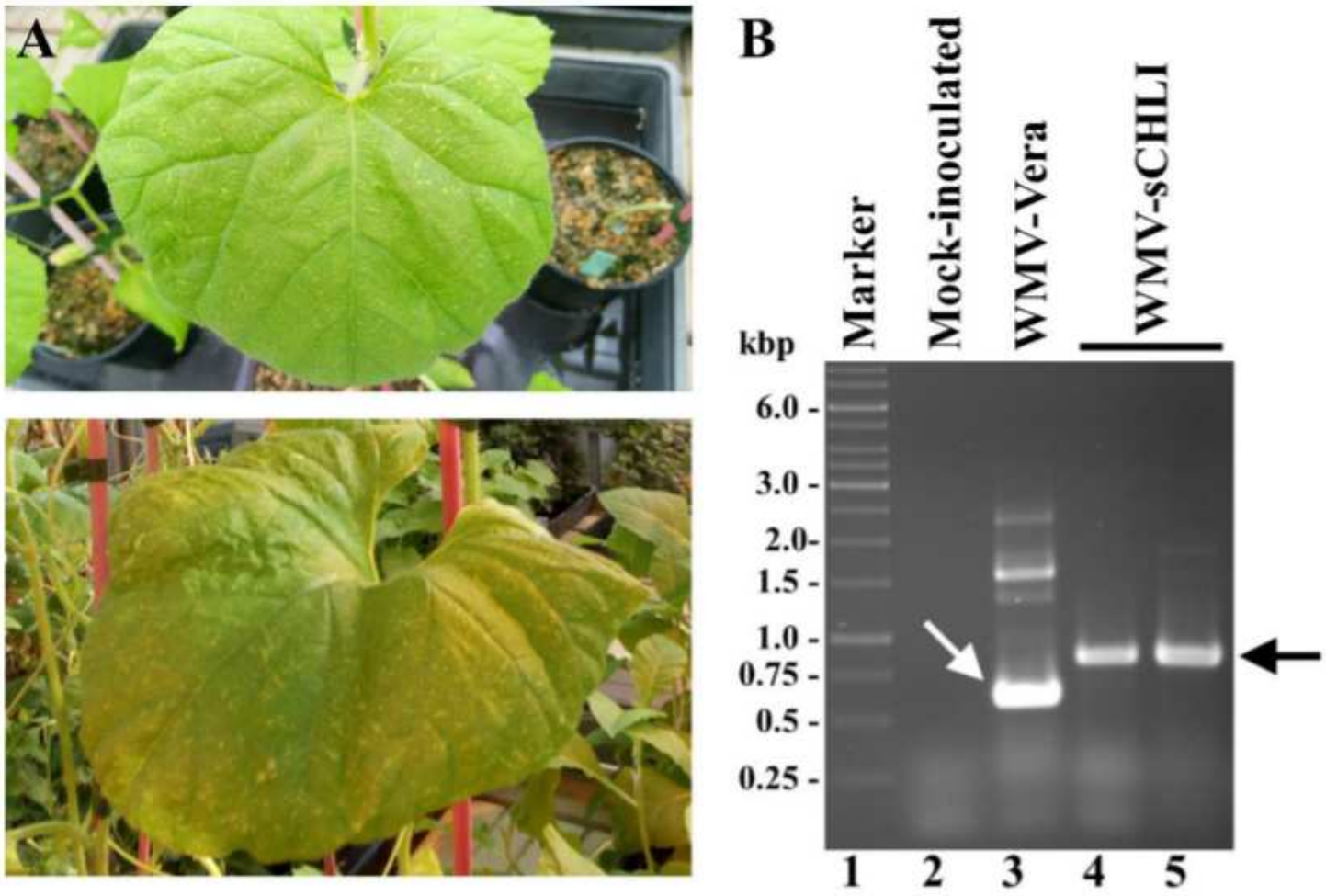

Figure 6

Analyses of melon plants inoculated with WMV-sCHLI. (A) Photographs were taken at 28 dpi of representative plants agroinoculated with WMV-sCHLI. (B) RT-PCR analysis of the inserted exogenous sequence at 21 dpi, as indicated in the legend for Fig. 3B. Lane 1, DNA marker with the sizes (in kbp) of some of the standards on the left; lanes 2 and 3, single representative plants mock-inoculated and inoculated with WMV-Vera; lanes 4 and 5, two representative plants inoculated with WMV-sCHLI.

Supplementary Files

This is a list of supplementary files associated with this preprint. Click to download.

- 20210208WMVbasedVIGScucurbitsSupplementaryMaterial.pdf